

Electrospun Ethyl-*p*-Methoxycinnamate Loaded CS/PEG/PLA Nanofibers

AATCC Journal of Research
2025, Vol. 12(1) 1–11
© The Author(s) 2025
Article reuse guidelines:
sagepub.com/journals-permissions
DOI: 10.1177/24723444241288284
journals.sagepub.com/home/aat



Do Thi Dinh^{1,2}, Ngo Thi Phuong³, Nguyen Thi Thu Thuy⁴,
Pham Thi Nhung³, Le Ngoc Hung^{5,6}, Do Thi Thanh Huyen³,
Nguyen Thai An¹, Jan Zidek⁷ and Le Minh Ha^{3,6} 

Abstract

In this study, the characteristic properties and biological activities of the electrospun nanofibers made of polymers including chitosan (CS), polyethylene glycol (PEG), and polylactic acid (PLA) loaded with 15% of a natural anti-inflammatory and analgesic agent, ethyl *p*-methoxycinnamate (EPMC), were reported. The morphological and chemical characteristics of the fibers were analyzed using a scanning electron microscope and Fourier transform infrared spectra, respectively. The mechanical properties and hydrophilicity of the nanofibers were also investigated. Research on the release of the bioactive compound EPMC from the nanofibers in phosphate-buffered saline medium showed that about 70% of EPMC was released after 24 h. The significant anti-inflammatory effect of the nanofibers was evaluated via inhibition of nitric oxide production in RAW264.7 cells stimulated by lipopolysaccharide with an IC₅₀ value of 41.05 ± 1.75 μg/mL. Besides, the nanofibers also exhibited anti-bacterial activity and were proved to be safe both *in vitro* and *in vivo*. The results suggested that the nanofibers CS/PEG/PLA loaded with ethyl *p*-methoxycinnamate may be a potential candidate for developing biomedical products related to inflammation.

Keywords

Anti-Inflammatory Effect, Chitosan, Electrospinning, Ethyl *p*-Methoxycinnamate, Nanofibers, Polyethylene Glycol, Polylactic Acid

Introduction

Electrospinning is a simple, low-cost, and effective technique for fabricating fibers with diameters ranging from micrometers to nanometers using a high-voltage power supply.¹ First introduced in 1900,² the electrospinning method has been developed and has undergone many revolutions over the past two decades,³ from the single-fluid blending process^{4–6} to bi-fluid coaxial electrospinning,^{7,8} side-by-side electrospinning,⁹ multiple-fluid triaxial,¹⁰ tri-layer Janus,^{11,12} and their combinations for producing new types of nanofibers.^{13,14} One merit of those complex nanostructures is the ability to tailor the multiple components for a certain joint effect. However, traditional single-fluid electrospinning can also be easily encapsulated with multiple components under reasonable selections of polymeric matrices, active ingredients and additives, and holds advantages for scale-up productions. Certainly, these multiple-

¹Hanoi University of Pharmacy, Hanoi, Vietnam

²Hai Duong Central College of Pharmacy, Hai Duong, Vietnam

³Institute of Natural Products Chemistry, Vietnam Academy of Science and Technology (VAST), Hanoi, Vietnam

⁴Phenikaa University Nano Institute (PHENA), Phenikaa University, Hanoi, Vietnam

⁵Center for High Technology Development, Vietnam Academy of Science and Technology (VAST), Hanoi, Vietnam

⁶Institute of Natural Products Chemistry, Vietnam Academy of Science and Technology (VAST), Hanoi, Vietnam

⁷Central European Institute of Technology (CEITEC), Brno University of Technology, Brno, Czech Republic

Date Received: 28 May 2024; Revised: 31 July 2024; Accepted: 2 August 2024

Corresponding author:

Le Minh Ha, Institute of Natural Products Chemistry, Vietnam Academy of Science and Technology (VAST), 18-Hoang Quoc Viet, Nghia Do, Cau Giay, Hanoi 100000, Vietnam.

Email: halm2vn@gmail.com; leminhha.inpc@gmail.com



Creative Commons Non Commercial CC BY-NC: This article is distributed under the terms of the Creative Commons

Attribution-NonCommercial 4.0 License (<https://creativecommons.org/licenses/by-nc/4.0/>) which permits non-commercial use,

reproduction and distribution of the work without further permission provided the original work is attributed as specified on the SAGE and Open Access pages (<https://us.sagepub.com/en-us/nam/open-access-at-sage>).

component nanofibers can also be designed into multi-chamber nanofibers in the future.¹⁵

Electrospun polymer nanofibers have been widely applied in various fields including drug delivery systems,^{16–19} tissue engineering,^{20–22} biosensors,^{23–26} wound dressings,^{27–30} filtration,^{31,32} and environmental engineering.^{33,34} One of the most important and extensively studied areas of electrospun polymer nanofibers is drug delivery.³³ A wide variety of drugs such as anti-inflammatory (ibuprofen,³⁴ naproxen,³⁵ indomethacin, griseofulvin,³⁶ meloxicam,³⁷ ketoprofen³⁸), anti-microbial (amoxicillin,³⁹ ciprofloxacin,⁴⁰ and tetracycline hydrochloride⁴¹), anti-cancer (doxorubicin⁴² and cisplatin⁴³), and anti-histamine (chlorpheniramine maleate⁴⁴) drugs have been loaded into the electrospun nanofibers to improve their bioavailability or to achieve controlled release.

Numerous organic polymers, including both natural and synthetic polymers, have been successfully explored for solution electrospinning to directly produce nanofibers.⁴⁵ Chitosan (CS), polylactic acid (PLA), and polyethylene glycol (PEG) are popular polymers that have been used for the fabrication of electrospun nanofibers. Chitosan is a natural polymer with biodegradable, biocompatible, anti-bacterial and anti-tumor effects, wound healing properties, and nontoxicity. The cationic nature of chitosan due to the presence of amino groups causes its characteristic properties and controlled drug release. Therefore, chitosan is currently being utilized in targeted drug delivery methods for the treatment of diverse diseases, including cancer, Crohn's disease, Alzheimer's disease, and Parkinson's disease. Some applications of chitosan involve drug delivery systems such as scaffolds, nanoparticles, hydrogels, nanocomposites, and fibers.^{46,47} However, the process of electrospinning pure chitosan presents significant difficulties and challenges due to various reasons including its restricted solubility in the majority of organic solvents, broad distribution of molecular weights, and three-dimensional networks of hydrogen bonds.^{4,33} Polylactic acid (PLA) is a polyester obtained from renewable resources such as beet, corn and sugar. Similar to chitosan, PLA is also biodegradable, biocompatible, bio-absorbable and non-toxic. PLA is one of the most promising materials used in the biomedical field, approved by the Food and Drug Administration for use in microcapsules, surgical sutures, microspheres, and implant materials. In contrast to chitosan, PLA has excellent mechanical strength and good fiber-forming ability. Some papers have shown that adding CS to PLA helps reduce the diameter of nanofibers by electrospinning technique.^{4,33} PEG is a hydrophilic, biocompatible polymer that has been extensively studied for its potential in various biomedical applications.⁴⁸

Nowadays, PEG has been widely utilized in drug delivery to enhance the stability and solubility of drugs *in vivo*, decrease clearance rates from circulation, and improve drug efficacy.⁴⁹ A previous report showed that the use of PEG in nanocomposite helps to enhance compatibility and dispersibility between PLA and CS and therefore improve the interaction between PLA and CS.⁵⁰

Kaempferia galanga L. is an important medicinal plant belonging to the family Zingiberaceae.⁵¹ In Vietnam, *K. galanga* has been used in some supplementary products and traditional medicines to treat inflammatory arthritis.⁵² Ethyl-*p* methoxycinnamate (EPMC), a natural potential anti-inflammatory and analgesic agent, was found to be the key compound that is responsible for the pharmacological properties of *K. galanga*.⁵³ The biological activities of EPMC were proved in both *in vitro* and *in vivo* models. EPMC strongly inhibited granuloma tissue formation in rats and dose-dependently inhibited carrageenan-induced edema with a minimum inhibitory concentration (MIC) value of 100 mg/kg. Moreover, EPMC was found to non-selectively inhibit the activities of cyclooxygenases 1 and 2, with IC₅₀ values of 1.12 μM and 0.83 μM, respectively. In another study, EPMC was reported to inhibit inflammation by suppressing interleukin-1, tumor necrosis factor-α both *in vivo* and *in vitro* models and inhibit angiogenesis by blocking endothelial functions *ex vivo*.^{54,55}

Nonsteroidal anti-inflammatory drugs (NSAIDs) are used widely to control inflammation and pain in different acute or chronic pain conditions such as osteoarthritis, rheumatoid arthritis, and other inflammatory diseases.^{56,57} However, NSAIDs can trigger various adverse effects on the gastrointestinal, hepatic, renal, and cardiovascular systems.^{56–59} Therefore, natural anti-inflammatory compounds like EPMC have become promising candidates for the treatment of inflammatory diseases due to their safety and lack of no side effects.^{60,61}

To create a new drug delivery system carrying the natural anti-inflammatory, analgesic agent EPMC for the treatment of inflammatory diseases, in the present study, we report the results of investigating the characteristic properties, anti-inflammatory and anti-bacterial effects, and safety of electrospun nanofibers made from polymers including CS, PEG, PLA loaded with 15% of EPMC.

Experimental

Materials

Chitosan (CS, M_w ≈ 100 kDa; degree of deacetylation = 99%) was purchased from Sigma-Aldrich (USA).

Poly(lactic acid) (PLA, $M_w = 200$ kDa), Poly(ethylene glycol) (PEG, $M_w = 600$ Da), acetic acid ($\geq 99.5\%$), chloroform ($\geq 99.5\%$), and ethanol ($\geq 99.5\%$) were purchased from Merck (Germany). EPMC ($\geq 95\%$) (obtained from *Kaempferia galanga*) was supplied by the Institute of Natural Products Chemistry, VAST, Vietnam. All the chemicals were used without further treatment.

Vero cells originated from the American Type Culture Collection (ATCC no. CCL-81.4), trichloroacetic acid (Alpha Chemika, India), sulforhodamine B (Sigma-Aldrich, USA), tris base solution (Alpha Chemika, India), ellipticine (Sigma-Aldrich, USA), and some other necessary chemicals were used for the cytotoxicity assay.

RAW 264.7 cells provided by Professor Domenico Delfino (Perugia University, Italy), lipopolysaccharides (LPS) from *Escherichia coli*, sodium nitrite, sulfanilamide, N-1-naphthyl ethylenediamine dihydrochloride, 3-(4,5-dimethylthiazole-2-yl)-2,5-diphenyl tetrazolium bromide (MTT), N^G -methyl-L-arginine acetate (L-NMMA), phosphoric acid and dimethyl sulphoxide (DMSO) from Sigma-Aldrich (USA), Dulbecco's Modified Eagle's Medium (DMEM), and fetal bovine serum (FBS) from Life Technologies (USA).

Bacterial strains including *E. coli* ATCC 25922, *Pseudomonas aeruginosa* ATCC 10145, *Bacillus subtilis* subsp. *spizizenii* ATCC 6633, *Staphylococcus aureus* subsp. *aureus* ATCC 25923, *Aspergillus niger* ATCC 6275, *Fusarium oxysporum* ATCC 7601, *Candida albicans* ATCC 10231, and *Saccharomyces cerevisiae* VTCC-Y-62 were obtained from the Experimental Biology Department, Institute of Natural Products Chemistry, VAST, Vietnam. These strains were maintained on nutrient agar and stored at 4°C.

Healthy white mice, weighing about 22–25 g, regardless of breed, were raised at the Institute of Biotechnology VAST, Vietnam under standard conditions of temperature and light for an acute toxicity assay.

Fabrication of Ethyl p-Methoxycinnamate-Loaded CS/PEG/PLA Nanofibers by Electrospinning

Preparation of Polymer Solutions for Each Electrospinning Batch. CS (0.1g) was completely dissolved in 5 mL of 90% acetic acid solution at 50°C to give CS solution at a concentration of 2% (w/v) (solution 1). PLA (0.75 g) and PEG (0.05 g) were dissolved in chloroform at 40°C to obtain a solution with concentrations of PLA and PEG of 15% and 1% (w/v), respectively (solution 2). A 0.159 g aliquot of EPMC was then added to solution 2

to achieve solution 3. Solution 1 was slowly added to solution 3 with stirring to obtain a homogeneous solution for electrospinning (solution 4).

Electrospinning Process. The horizontal electrospinning process was carried out using an electrospinning machine. Solution 4 was put into a 5 mL syringe attached to a metal needle that was connected to a high voltage of 20 kV. The feeding rate of the solution was 1 mL/h. The distance from the needle to the drum collector was set at 15 cm. The thickness of the nanofibers was controlled through the electrospinning time. The produced nanofibers containing 15% EPMC were dried by a vacuum drying machine at 50°C for 12 h to completely remove the solvents.

Characterization of the Nanofibers

Morphological Analysis. The morphological characteristics of the electrospun nanofibers were observed using a scanning electron microscope (Hitachi, S-4800). The diameter of nanofibers was determined using image processing software (ImageJ). The average diameter was then calculated randomly from about 100 nanofibers using MS Excel software.

Chemical Analysis. Chemical characterization of the nanofibers was observed using an FT-IR spectrometer (GXPerkinElmer, USA).

Mechanical Analysis. The tensile strength of the nanofibers was measured using a material testing machine Zwick Z2.5 (Germany). Each sample was cut to dimensions of 15 mm in width and 50 mm in length. The sample's thickness was the mean thickness value at three different positions on the sample measured by a digital micrometer. The test speed was 10 mm/min, and the gauge length was 30 mm. The measurements were repeated three times.

Wetting Study. The wetting properties of the nanofibers were tested by the sessile drop method using optical contact angle equipment Dataphysics OCA 50 (Germany). A small droplet (5 μ L) of deionized water was placed on the surface of the nanofibers. The contact angle was measured using a digital camera at 60 s after the droplet touched the nanofiber surface. This measurement was repeated three times.

In Vitro EPMC Release Study

The *in vitro* EPMC release from the nanofibers was evaluated using a UV-vis spectrometer (EMC-61PCS-UV spectrophotometer). The nanofibers (10 mg) were

immersed in 100 mL of phosphate-buffered saline (PBS) buffer solution (pH 7.4) and kept at 37°C, with magnetic stirring. At specific times (0.5, 1.0, 1.5, 2.0, 2.5, 3.0, 4.0, 8.0, 12.0, 16.0, 20.0, and 24.0 h), each 3 mL of supernatant solution was withdrawn and replaced by an equal amount of fresh PBS solution. The samples were centrifuged and filtered to give the supernatant layer, which was then analyzed for absorbance at a wavelength of 310 nm. The calibration curve of EPMC was obtained by measuring different concentrations of EPMC in PBS in the same condition (pH 7.4, 37°C, magnetic stirring, λ_{\max} 310 nm). The percentage of EPMC released was calculated according to equation (1):

$$\text{EPMC release (\%)} = \frac{Mt}{Mo} \times 100\% \quad (1)$$

where Mt calculated from the calibration curve is the amount of EPMC released up to time t , and Mo is the total amount of EPMC loaded in the nanofibers. Each experiment was performed in triplicate to get the average value.

Nitrite Assay

Initially, RAW264.7 cells were cultured in DMEM medium supplemented with 10% FBS in 96-well plates with a density of 2×10^5 cells per well. The cells were then incubated in a humidified atmosphere with 5% CO₂ at 37°C for 24 h. Subsequently, the medium was replaced with DMEM (free FBS) and incubated for an additional 3 h. The cells were treated with test samples for 2 h, followed by treatment with 1 $\mu\text{g/mL}$ of LPS for 24 h. To assess the production of nitric oxide, the accumulated nitrite in the culture medium was measured using the Griess reaction. In brief, 100 μL of the culture medium was mixed with 100 μL of Griess reagent which consisted of 50 μL of 1% (w/v) sulfanilamide in 5% (v/v) phosphoric acid and 50 μL of 0.1% (w/v) *N*-1-naphthyl ethylenediamine dihydrochloride. This mixture was then incubated for 10 min at room temperature. The optical density of the mixture after the Griess reaction was measured at 540 nm using an ELISA reader. The sample's ability to inhibit NO production was determined by formula (2):

$$\text{Inhibition (\%)} = 100\% - \frac{\text{OD}(\text{sample})}{\text{OD}(\text{LPS})} \times 100\% \quad (2)$$

where OD (sample) is the absorbance in wells treated with the test sample and OD (LPS) is the absorbance in wells of LPS-stimulated nitric oxide (NO) production.

The test was repeated three times to ensure accuracy. The IC₅₀ value was determined using TableCurve 2Dv4

software. The DMEM (free FBS) medium was used as a blank, and L-NMMA was used as the positive control with a concentration range of 100–20–4–0.8 $\mu\text{g/mL}$. The remaining cells in the cultured 96-well plates were subjected to an MTT assay to evaluate cell viability.⁶²

Anti-bacterial Assay

The anti-bacterial activity of the nanofibers was conducted on 96-well microplates according to the methods of Vlietinck⁶³ and Mekane and Kandel.⁶⁴ Test bacterial strains included *E. coli* ATCC 25922, *P. aeruginosa* ATCC 10145 (Gram-negative), *B. subtilis* subsp. *spizizenii* ATCC 6633, *S. aureus* subsp. *aureus* ATCC 25923 (Gram-positive), *A. niger* ATCC 6275, *F. oxysporum* ATCC 7601 (filamentous fungi), *C. albicans* ATCC 10231, and *S. cerevisiae* VTCC-Y-62 (yeast). Streptomycin, tetracycline, and nystatin were used as positive controls. The microplates were incubated for 24 h at 37°C for bacteria and 48 h at 30°C for fungi. The lowest concentration of the fibers that inhibited the visible growth of a microorganism (MIC) after incubation was observed and recorded.

Cytotoxicity Assay

Vero cells were cultured at 37°C in DMEM medium supplemented with 10% FBS, 100 U/mL penicillin, and 100 $\mu\text{g/mL}$ streptomycin in a 5% CO₂ incubator. The *in vitro* cytotoxicity assay was performed according to the method of Skehan et al.⁶⁵ Vero cells were seeded (1×10^4 cells per well in 96-well plates) at the exponential growth phase and treated with serially diluted concentrations (400, 200, 100, 50, and 25 $\mu\text{g/mL}$) of the nanofibers in DMSO. After 72 h of incubation (37°C, 5% CO₂), cells were fixed with trichloroacetic acid and stained with 0.4% sulforhodamine B. The amount of dissolved cell binding dye in tris base solution was detected by absorbance (optical density) at 540 nm using a microplate reader. Wells containing Vero cells without test samples were used as day 0 controls. The effect of the test sample on Vero cells was expressed as the cell survival (CS) percentage according to the following formula:

$$\text{CS (\%)} = \frac{\text{OD}(\text{sample}) - \text{OD}(\text{day 0})}{\text{OD}(\text{DMSO}) - \text{OD}(\text{day 0})} \quad (3)$$

where OD (sample) is the absorbance in wells treated with the test sample, OD (DMSO) is the absorbance in wells treated with DMSO, and OD (day 0) was the absorbance in the control well on day 0.

The cell survival (CS) percentage is presented as the mean \pm SD of three replications. Ellipticine, a highly cytotoxic substance, was used as a positive control in the experiment.

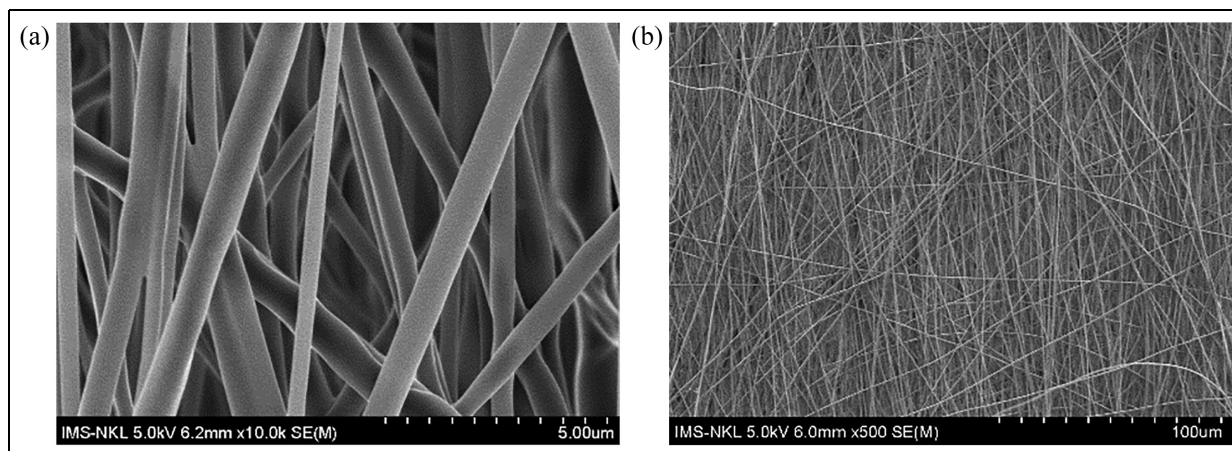


Figure 1. SEM micrographs of the nanofibers at different magnifications: (a) $\times 10,000$ and (b) $\times 500$.

Acute Toxicity Assay

Acute toxicity was conducted according to Organisation for Economic Co-operation and Development (OECD) guideline number 420 and the Guidelines for pre-clinical and clinical testing of oriental medicines and medicinal herbs issued by the Vietnam Ministry of Health under Decision No. 141/QD-K2DT dated October 27, 2015.^{66,67} The care and use of laboratory animals in this study were conducted according to ethical guidelines and approval from the Scientific Council of the Institute of Biotechnology, VAST for animal studies dated December 4, 2023. The nanofibers were ground into powder as the sample for the acute toxicity test.

Preliminary test: 10 white mice were completely starved for 16 h before receiving the sample at the highest dose of 10,000 mg/kg body weight. In the case where no mice died within 24 h of observation and monitoring, the official test would be immediately conducted according to the fixed-dose procedure.

Official test: 20 white mice were divided into two groups (10 mice/group) and completely starved for 16 h before receiving the sample. Group 1 (control group) was treated with distilled water. Group 2 was orally administered the sample at a dose of 5000 mg/kg body weight. Treated mice were observed continuously for the first 2 h. Their food and water consumption, body weight, death, and reaction to light and sound were monitored and recorded for 14 days.

Statistical Analysis

The data were processed by Excel software. The results are presented as mean \pm SD (standard deviation). A *t*-test was used for statistical comparison between different groups. The differences with $p < 0.05$ were considered statistically significant.

Results and Discussion

Characterization of the Nanofibers Loaded With Ethyl *p*-Methoxycinnamate

The nanofibers made from three polymers, CS, PEG, and PLA loaded with 15% EPMC (w/w), were produced by the electrospinning method. The selected content of EPMC in the nanofibers was the highest content at which the electrospun nanofiber formation process went smoothly. At contents of EPMC more than 15%, the produced nanofibers had beads and the fiber formation process was interrupted because the injector of the electrospinning machine was clogged. Figure 1 shows that the surface of the nanofibers loaded with 15% EPMC was smooth and uniform, without any beads. The average diameter of the nanofibers was 224 ± 66 nm.

Figure 2 presents the FT-IR spectra of CS, PEG, PLA, and EPMC, and the nanofibers. The FT-IR spectrum of EPMC shows some typical absorption peaks at 1700 cm^{-1} (C=O), 1167 cm^{-1} (C-O), $2978\text{--}2841\text{ cm}^{-1}$ (C-H), and $1627\text{--}1508\text{ cm}^{-1}$ (aromatic C=C). The absorption at 825 cm^{-1} suggests the presence of para-substitution in the EPMC molecules. The FT-IR spectrum of CS reveals the strong broad absorption band around 3361 cm^{-1} corresponding to N-H and O-H stretching vibrations, the peak at 2869 cm^{-1} assigned to C-H stretching vibrations, and the strong doublet absorption peak at 1023 and 1066 cm^{-1} attributed to the pyranose structure.⁶⁸ The FT-IR spectrum of PEG exhibited two sharp peaks at 1089 cm^{-1} (C-O) and 2878 cm^{-1} (C-H). The FT-IR spectrum of PLA displayed characteristic stretching frequencies for C=O, C-H, and C-O at 1747 , 2994 , 2944 , and 1080 cm^{-1} , respectively. All the above peaks of the components were observed in the FT-IR spectrum of the nanofibers. This suggested the presence of EPMC, CS, PEG, and



Figure 2. FT-IR spectra of CS (A), PEG (B) PLA (C), EPMC (D), and the nanofibers (E).

PLA in the nanofibers. However, there were certain shifts of these peaks on the spectrum of the nanofibers, which suggested interactions among these constituents in the nanofibers. The two strongest shifted peaks observed in the spectrum of the nanofibers were 1752 and 1085 cm^{-1} corresponding to the C=O and C-O bonds.

Mechanical analysis of the nanofibers (thickness of $120 \pm 4.6\ \mu\text{m}$) exhibited a tensile strength of $2.07 \pm 0.56\text{ MPa}$, an elongation at break of $13.55 \pm 2.27\%$, and a Young's modulus of $106.31 \pm 24.02\text{ MPa}$. The stress-strain diagram of the nanofibers (Figure 3) describes two stages of the tensile process. A is considered the moment at which the bonds between fibers begin to break, whereas B is the point at which the nanofiber mat breaks completely.⁶⁹ Tensile strength is believed to be proportional to the thickness of the material.⁷⁰ Hence, it is possible to improve the mechanical properties of the nanofibers by increasing the thickness of the produced nanofibers.

The significance of wettability in enhancing the release of active ingredients and the dissolution of pharmaceuticals is widely acknowledged.⁷¹ The water contact angle was used to evaluate the hydrophilicity of the nanofibers. The nanofibers were found to be hydrophilic with a contact angle of $73.1 \pm 0.8^\circ$.

In Vitro Drug Release Study

The medium used for studying EPMC release from the nanofibers was PBS (pH 7.4), with the same pH value as the terminal ileum and plasma.¹⁷ Three mechanisms can be used to describe drug release from nanofibers.

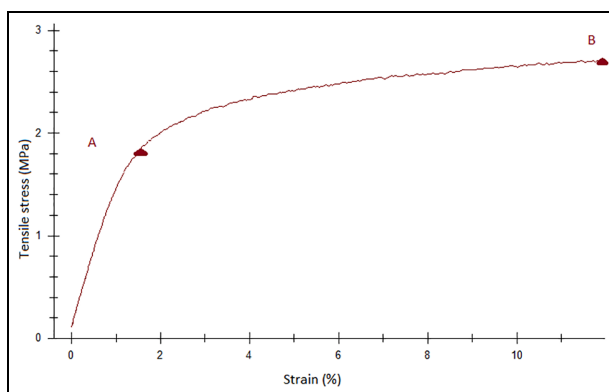


Figure 3. The stress-strain diagram of the nanofibers. A: the Yield point, B: the Breaking point.

These mechanisms include desorption from the surface of the fibers, solid-state diffusion through the fibers, and degradation of the fibers *in vivo*.⁷² The percentage of EPMC released from the nanofibers over time in hours is presented in Figure 4. The graph shows that the EPMC release characteristics from nanofibers can be divided into two distinct phases. The first phase is an initial burst release, where a significant amount of EPMC (61.36%) is released within 4 h. The second phase had very little fluctuation in the percentage of EPMC released after the initial 4 h period. The burst release of EPMC might be attributed to the release of EPMC at the surface area of nanofibers. Sustained drug release may be maintained by diffusion of EPMC through solid nanofibers. Perhaps H-bond interactions between EPMC molecules and functional groups of the polymers contribute to give sustained release of

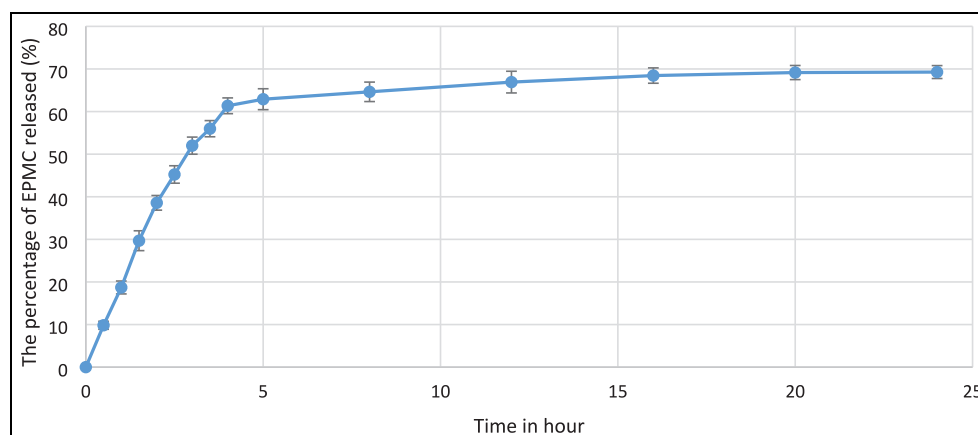


Figure 4. EPMC release from the nanofibers.

Table 1. Inhibition of NO production of the nanofibers in LPS-stimulated RAW264.7 cells.

| Sample | Concentration ($\mu\text{g/mL}$) | NO inhibition (%) | Cell survival (%) | IC ₅₀ ($\mu\text{g/mL}$) |
|---------------------------------|------------------------------------|-------------------|-------------------|---------------------------------------|
| The nanofibers loaded with EPMC | 60 | 90.30 \pm 1.67 | 85.39 \pm 1.35 | 41.05 \pm 1.75 |
| | 50 | 64.74 \pm 2.72 | 98.68 \pm 1.90 | |
| | 40 | 50.64 \pm 0.91 | 99.76 \pm 1.23 | |
| | 30 | 31.09 \pm 0.56 | 99.81 \pm 1.08 | |
| | 20 | 17.41 \pm 0.93 | 99.98 \pm 1.15 | |
| Positive control (L-NMMA) | | | | 9.11 \pm 1.02 |

EPMC. As a result, the nanofibers release about 70% of EPMC after 24 h. Incomplete drug release of EPMC may be due to the drug being trapped inside the polymer matrix. In some previous studies,^{73–77} similar incomplete drug release profiles were reported. For example, about 60% of curcumin was released from zein/silk fibroin/chitosan nanofibers loaded with curcumin in the first 15 h (burst release), and 79% of curcumin was released after 96 h (sustained release).⁷⁷ Complete drug release can be achieved through nanofiber biodegradation.⁷²

Anti-Inflammatory Effect

Nitric oxide (NO) is a crucial signaling molecule involved in the pathogenesis of inflammation. Under normal physiological conditions, NO can give anti-inflammatory effects. However, it is also an inflammatory mediator during inflammation. Overproduction of NO as an inflammatory mediator can lead to tissue destruction. Therefore, inhibitors of NO production are considered one of the important targets in the control of inflammatory diseases.⁷⁸ In the current study, we evaluated the anti-inflammatory properties of the nanofibers loaded with EPMC via the inhibition of NO production in LPS-stimulated RAW264.7 cells. The results (Table 1) showed that the nanofibers exhibited

significant inhibitory activity on NO production with an IC₅₀ value of 41.05 \pm 1.75 $\mu\text{g/mL}$ and did not affect the viability of RAW264.7 cells at test concentrations (cell survival rate > 80%). On the other hand, the inhibitory effect on NO production in human macrophage cells (U937) of free EPMC was previously reported to be 23.8% at a concentration of 200 $\mu\text{g/mL}$.⁵⁵

Anti-bacterial Effect

Natural products with MIC values below 1 mg/mL are considered to have noteworthy anti-bacterial activity.⁷⁹ The results (Table 2) showed that the nanofibers exhibited anti-bacterial effect against four types of microorganisms: *C. albicans* ATCC 10231, *E. coli* ATCC 25922 (MIC value of 100 $\mu\text{g/mL}$), *P. aeruginosa* ATCC 10145 (MIC value of 200 $\mu\text{g/mL}$), and *A. niger* ATCC 6275 (MIC value of 400 $\mu\text{g/mL}$). However, the nanofibers did not show inhibitory ability against the other four microbial strains at the tested concentrations.

Cytotoxicity Study

Vero cells obtained from African green monkey kidneys are similar to human cells and can be easily cultured.⁸⁰ The Vero cell line is frequently utilized as a normal cell

Table 2. Anti-microbial effects of the nanofibers.

| No. | Microorganism | MIC ($\mu\text{g/mL}$) |
|-----|---|--------------------------|
| 1 | <i>Escherichia coli</i> ATCC 25922 | 100 |
| 2 | <i>Pseudomonas aeruginosa</i> ATCC 10145 | 200 |
| 3 | <i>Bacillus subtilis</i> subsp. <i>spizizenii</i> ATCC 6633 | (-) |
| 4 | <i>Staphylococcus aureus</i> subsp. <i>aureus</i> ATCC 25923 | 400 |
| 5 | <i>Aspergillus niger</i> ATCC 6275 | (-) |
| 6 | <i>Fusarium oxysporum</i> ATCC 7601 | (-) |
| 7 | <i>Candida albicans</i> ATCC 10231 | 100 |
| 8 | <i>Saccharomyces cerevisiae</i> VTCC-Y-62 | (-) |

Note: (-): the nanofibers did not show inhibitory ability against microbial strains at the tested concentrations.

line control for assessing the *in vitro* cytotoxicity of substances against normal cells.⁸¹ The results of the cell viability assay on Vero cells (Table 3) showed that the nanofibers did not exhibit cytotoxic activity on the Vero cell line at the maximum concentration of 400 $\mu\text{g/mL}$ with a cell survival of $97.91 \pm 0.73\%$. This suggested that the nanofibers would be safe due to having no effects on normal cells in the *in vitro* study.

Acute Toxicity

In the acute study, oral administration of the nanofibers sample at a dose of 5000 mg/kg body weight did not cause any death or signs of toxicity in mice during the experimental period of 14 days. After being treated with the sample, experimental animals still moved and ate normally and responded to light and sound well. There was no significant difference in body weight between the control group and the experimental group ($p > 0.05$). According to the classification of oral toxins by the Globally Harmonized System of Classification and Labeling of Chemicals (GHS) and OECD, the nanofibers at a dose of 5000 mg/kg body weight were considered to be safe and did not cause acute toxicity in mice orally. The dose can be used as a basis for dose calculation for further pharmacological studies.

Conclusion

In the current article, the EPMC (15%, w/w) loaded CS/PEG/PLA nanofibers were fabricated with an average fiber diameter of about 224 ± 66 nm. The mechanical and physicochemical properties of the fibers were also evaluated. Research on EPMC release in PBS medium showed that after 24 h, about 70% of EPMC was released from the nanofibers. The nanofibers revealed significant anti-inflammatory activity via the inhibition of NO production with an IC_{50} value of 41.05 ± 1.75 $\mu\text{g/mL}$, along with anti-bacterial activities.

Table 3. The results of cell viability assay.

| No. | Concentration ($\mu\text{g/mL}$) | Cell survival (%) |
|-----|------------------------------------|-------------------|
| 1 | 400 | 97.91 ± 0.73 |
| 2 | 200 | 98.89 ± 0.78 |
| 3 | 100 | 98.96 ± 0.99 |
| 4 | 50 | 99.53 ± 0.87 |
| 5 | 25 | 99.87 ± 1.03 |

In addition, the nanofibers loaded with EPMC were proved to be safe via both *in vitro* and *in vivo* levels. This is the first time, the anti-inflammatory and analgesic compound EPMC has been loaded in a polymeric matrix by electrospinning, and the characteristics and biological activities of the nanofibers have been reported. The initial research findings of EPMC-loaded CS/PEG/PLA nanofibers suggested that the fibers would be a potential candidate for developing biomedical products for the treatment of inflammatory diseases. Further in-depth studies on the *in vivo* anti-inflammatory effect and safety of the nanofibers should be conducted in the future to provide more scientific evidence for the application of the fibers in the biomedical field.


Declaration of conflicting interests

The author(s) declared no potential conflicts of interest with respect to the research, authorship, and/or publication of this article.

Funding

The author(s) disclosed receipt of the following financial support for the research, authorship, and/or publication of this article: This work was performed under the financial support of Vietnam–Czech Republic joint research project (grant no. NT/CZ/23/07).

ORCID iD

Le Minh Ha  <https://orcid.org/0000-0002-2173-1393>

References

1. Park JS. Electrospinning and its applications. *ANSN* 2010; 1(4): 043002.
2. Cooley JF. Improved methods of and apparatus for electrically separating the relatively volatile liquid component from the component of relatively fixed substances of composite fluids. Patent 6385-19, 1990.
3. Li Y, Zhu J, Cheng H, et al. Developments of advanced electrospinning techniques: A critical review. *Adv Mater Technol* 2021; 6(11): 2100410.
4. Hardiansyah A, Tanadi H, Yang MC, et al. Electrospinning and antibacterial activity of chitosan-blended poly (lactic acid) nanofibers. *J Polym Res* 2015; 22: 1–10.

5. Trang MTT, Thuy NTT, Duong LQ, et al. A novel nanofiber Cur-loaded polylactic acid constructed by electrospinning. *ANSN* 2012; 3(2): 025014.
6. Thomas MS, Pillai PK, Faria M, et al. Electrospun polylactic acid–chitosan composite: A bio-based alternative for inorganic composites for advanced application. *J Mater Sci: Mater Med* 2018; 29: 1–12.
7. Huang C, Wang M, Yu S, et al. Electrospun fenoprofen/polycaprolactone @ tranexamic acid/hydroxyapatite nanofibers as orthopedic hemostasis dressings. *Nanomater* 2024; 14(7): 646.
8. Ali A, Bhuiyan MR, Mohebbullah M, et al. Nigella sativa embedded co-axial electrospun PVA–collagen composite nanofibrous membrane for biomedical applications. *AATCC J Res* 2024; 11: 263–272.
9. Zhang Z, Zhang Y, Guo Y, et al. Preparing gelatin-containing polycaprolactone/polylactic acid nanofibrous membranes for periodontal tissue regeneration using side-by-side electrospinning technology. *J Biomater Appl* 2024; 39(1): 48–57.
10. Wang M, Hou J, Yu DG, et al. Electrospun tri-layer nanodepots for sustained release of acyclovir. *J Alloys Compd* 2020; 846: 156471.
11. Zhao P, Zhou K, Xia Y, et al. Electrospun trilayer eccentric Janus nanofibers for a combined treatment of periodontitis. *Adv Fiber Mater* 2024; 6: 1053–1073.
12. Xu L, Li Q, Wang H, et al. Electrospun multi-functional medicated tri-section Janus nanofibers for an improved anti-adhesion tendon repair. *Chem Eng J* 2024; 492: 152359.
13. Yu DG, Gong W, Zhou J, et al. Engineered shapes using electrohydrodynamic atomization for an improved drug delivery. *Wiley Interdiscip Rev Nanomed Nanobiotechnol* 2024; 16(3): e1964.
14. Sun Y, Zhou J, Zhang Z, et al. Integrated Janus nanofibers enabled by a co-shell solvent for enhancing icariin delivery efficiency. *Int J Pharm* 2024; 658: 124180.
15. Keirouz A, Wang Z, Reddy VS, et al. The history of electrospinning: Past, present, and future developments. *Adv Mater Technol* 2023; 8(11): 2201723.
16. Cleaton C, Keirouz A, Chen X, et al. Electrospun nanofibers for drug delivery and biosensing. *ACS Biomater Sci Eng* 2019; 5(9): 4183–4205.
17. Uhljar LE, Kan SY, Radacs N, et al. In vitro drug release, permeability, and structural test of ciprofloxacin-loaded nanofibers. *Pharmaceutics* 2021; 13(4): 556.
18. Torres MEJ, Cornejo BJM, Serrano MA, et al. A summary of electrospun nanofibers as drug delivery system: Drugs loaded and biopolymers used as matrices. *Curr Drug Deliv* 2018; 15(10): 1360–1374.
19. Kendre PN, Gite M, Jain SP, et al. Nanocomposite polymeric materials: State of the art in the development of biomedical drug delivery systems and devices. *Polym Bull* 2022; 79(11): 9237–9265.
20. Xie J, Ewan MRM, Schwartz AG, et al. Electrospun nanofibers for neural tissue engineering. *Nanoscale* 2010; 2(1): 35–44.
21. Huang T, Zeng Y, Li C, et al. Application and development of electrospun nanofiber scaffolds for bone tissue engineering. *ACS Biomater Sci Eng* 2024; 10(7): 4114–4144.
22. Wu J, Yu F, Shao M, et al. Electrospun nanofiber scaffold for skin tissue engineering: A review. *ACS Appl Bio Mater* 2024; 7(6): 3556–3567.
23. Kang S, Zhao K, Yu DG, et al. Advances in biosensing and environmental monitoring based on electrospun nanofibers. *Adv Fiber Mater* 2022; 4(3): 404–435.
24. Shariatzadeh FJ, Logsetty S and Liu S. Ultrasensitive nanofiber biosensor: Rapid in situ chromatic detection of bacteria for healthcare innovation. *ACS Appl Bio Mater* 2024; 7(4): 2378–2388.
25. Gawali CR, Daweshar E, Kolhe A, et al. Recent advances in nanostructured conducting polymer electrospun for application in electrochemical biosensors. *Microchem J* 2024; 200: 110326.
26. Liu J, Dong Z, Huan K, et al. Application of the electrospinning technique in electrochemical biosensors: An overview. *Molecules* 2024; 29(12): 2769.
27. Li M, Qiu W, Wang Q, et al. Nitric oxide-releasing tryptophan-based poly (ester urea)s electrospun composite nanofiber mats with antibacterial and antibiofilm activities for infected wound healing. *ACS Appl Mater Interfaces* 2022; 14(14): 15911–15926.
28. Zhang X, Lv R, Chen L, et al. A multifunctional janus electrospun nanofiber dressing with biofluid draining, monitoring, and antibacterial properties for wound healing. *ACS Appl Mater Interfaces* 2022; 14(11): 12984–13000.
29. Abrigo M, McArthur SL and Kingshott P. Electrospun nanofibers as dressings for chronic wound care: Advances, challenges, and future prospects. *Macromol Biosci* 2014; 14(6): 772–792.
30. Miguel SP, Figueira DR, Simões D, et al. Electrospun polymeric nanofibres as wound dressings: A review. *Colloids Surf B Biointerfaces* 2018; 169: 60–71.
31. Liu H, Zhu Y, Zhang C, et al. Electrospun nanofiber as building blocks for high-performance air filter: A review. *Nano Today* 2024; 55: 102161.
32. Wang X, Wang Q, Zhang W, et al. Polyvinylidene fluoride-co-hexafluoropropyle electrospun nanofiber membranes for PM0. 3 filtration. *ACS Appl Nano Mater* 2024; 7(9): 10216–10225.
33. Hu X, Liu S, Zhou G, et al. Electrospinning of polymeric nanofibers for drug delivery applications. *J Control Release* 2014; 185: 12–21.
34. Yu DG, Shen XX, Branford WC, et al. Oral fast-dissolving drug delivery membranes prepared from electrospun polyvinylpyrrolidone ultrafine fibers. *Nanotechnology* 2019; 20(5): 055104.
35. Wu YH, Yu DG, Li HC, et al. Electrospun nanofibers for fast dissolution of naproxen prepared using a coaxial process with ethanol as a shell fluid. *AMM* 2014; 662: 29–32.
36. Lopez FL, Shearman GC, Gaisford S, et al. Amorphous formulations of indomethacin and griseofulvin prepared by electrospinning. *Mol Pharmaceutics* 2014; 11(12): 4327–4338.
37. Samprasit W, Akkaramongkolporn P, Ngawhirunpat T, et al. Fast releasing oral electrospun PVP/CD nanofiber mats of taste-masked meloxicam. *Int J Pharm* 2015; 487(1–2): 213–222.

38. Kenawy ER, Abdel HFI, Newehy MHE, et al. Controlled release of ketoprofen from electrospun poly (vinyl alcohol) nanofibers. *Mater Sci Eng A* 2007; 459(1–2): 390–396.
39. Ortega MMC, Montaña FAG, Rodríguez FDE, et al. Amoxicillin embedded in cellulose acetate-poly (vinyl pyrrolidone) fibers prepared by coaxial electrospinning: Preparation and characterization. *Mater Lett* 2012; 76: 250–254.
40. Modgill V, Garg T, Goyal AK, et al. Permeability study of ciprofloxacin from ultra-thin nanofibrous film through various mucosal membranes. *Artif Cells Nanomed Biotechnol* 2016; 44(1): 122–127.
41. He CL, Huang ZM, Han XJ, et al. Coaxial electrospun poly (L-lactic acid) ultrafine fibers for sustained drug delivery. *J Macromol Sci B* 2006; 45(4): 515–524.
42. Xu X, Yang L, Xu X, et al. Ultrafine medicated fibers electrospun from W/O emulsions. *J Control Release* 2005; 108(1): 33–42.
43. Zhang Y, Liu S, Wang X, et al. Prevention of local liver cancer recurrence after surgery using multilayered cisplatin-loaded polylactide electrospun nanofibers. *Chinese J Polym Sci* 2014; 32(8): 1111–1118.
44. Jaiturong P, Sirithunyalug B, Eitsayeam S, et al. Preparation of glutinous rice starch/polyvinyl alcohol copolymer electrospun fibers for using as a drug delivery carrier. *Asian J Pharm Sci* 2018; 13(3): 239–247.
45. Xue J, Wu T, Dai Y, et al. Electrospinning and electrospun nanofibers: Methods, materials, and applications. *Chem Rev* 2019; 119(8): 5298–5415.
46. Hasnain MS, Beg S and Nayak AK. *Chitosan in drug delivery*. Cambridge: Academic Press, 2021, pp. 4–11.
47. Aranaz I, Alcántara AR, Civera MC, et al. Chitosan: An overview of its properties and applications. *Polymers* 2021; 13(19): 3256.
48. Xu XL, Zhou GQ, Li XJ, et al. Solution blowing of chitosan/PLA/PEG hydrogel nanofibers for wound dressing. *Fiber Polym* 2016; 17: 205–211.
49. Hoang TTT, Pilkington EH, Nguyen DH, et al. The importance of poly (ethylene glycol) alternatives for overcoming PEG immunogenicity in drug delivery and bioconjugation. *Polymers* 2020; 12(2): 298.
50. Trang NTT, Chinh NT, Giang NV, et al. Hydrolysis of green nanocomposites of poly (lactic acid) (PLA), chitosan (CS) and polyethylene glycol (PEG) in acid solution. *Green Process Synth* 2016; 5(5): 443–449.
51. Khairullah AR, Solikhah TI, Ansori ANM, et al. Medicinal importance of *Kaempferia galanga* L. (Zingiberaceae): A comprehensive review. *J Herbmed Pharmacol* 2021; 10(3): 281–288.
52. Loi DT. *Vietnamese medicinal plants and herbs*. Hanoi: Medical Publishing House, 2004, pp. 365–366 (in Vietnamese).
53. Shetu HJ, Trisha KT, Sikta SA, et al. Pharmacological importance of *Kaempferia galanga* (Zingiberaceae): A mini review. *IJRPS* 2018; 3(3): 32–39.
54. Umar MI, Asmawi MZ, Sadikun A, et al. Bioactivity-guided isolation of ethyl-*p*-methoxycinnamate, an anti-inflammatory constituent from *Kaempferia galanga* L. extracts. *Molecules* 2012; 17(7): 8720–8734.
55. Umar MI, Asmawi MZ, Sadikun A, et al. Ethyl-*p*-methoxycinnamate isolated from *Kaempferia galanga* inhibits inflammation by suppressing interleukin-1, tumor necrosis factor- α , and angiogenesis by blocking endothelial functions. *Clinics* 2014; 69: 134–144.
56. Keller CL, Jones NT, Abadie RB, et al. Non-steroidal anti-inflammatory drug (NSAID)-, potassium supplement-, bisphosphonate-, and doxycycline-mediated peptic ulcer effects: A narrative review. *Cureus* 2024; 16(1): e51894.
57. Tolba R. Nonsteroidal anti-inflammatory drugs (NSAIDs). In: Pope J and Deer T (eds) *Treatment of chronic pain conditions*. New York: Springer, 2017, pp. 77–79.
58. Vonkeman HE and Laar MAF. Nonsteroidal anti-inflammatory drugs: Adverse effects and their prevention. *Semin Arthritis Rheum* 2010; 39(4): 294–312.
59. Rainsford KD. Profile and mechanisms of gastrointestinal and other side effects of nonsteroidal anti-inflammatory drugs (NSAIDs). *Am J Med* 1999; 107(6): 27–35.
60. Vasconcelos F, Lima AC, Bonani W, et al. Microfluidic-assisted electrospinning, an alternative to coaxial, as a controlled dual drug release system to treat inflammatory arthritic diseases. *Biomater Adv* 2022; 134: 112585.
61. Elshabrawy HA, Dena ASA and El-Sherbiny IM. Triple-layered platform utilizing electrospun nanofibers and 3D-printed sodium alginate-based hydrogel for effective topical treatment of rheumatoid arthritis. *Int J Bio Macromol* 2024; 259: 129195.
62. Van MJ, Kaspers GJ and Cloos J. Cell sensitivity assays: The MTT assay. In: Cree IA (ed.) *Cancer cell culture: Methods and protocols*. Totowa, NJ: Humana Press, 2011, pp. 237–245.
63. Vlietinck AJ. Screening methods for detection and evaluation of biological activities of plant preparations. In: Bohlin L and Bruhn JG (eds) *Bioassay methods in natural product research and drug development*. Dordrecht: Springer, 1999, pp. 37–52.
64. McKane L and Kandel J. Bacterial growth and laboratory cultivation. In: Prancan KM, Cloud D and Castellano E (eds) *Microbiology essentials and applications*. New York: McGraw-Hill, 1996, pp. 97–125.
65. Skehan P, Storeng R, Scudiero D, et al. New colorimetric cytotoxicity assay for anticancer-drug screening. *JNCI – J Natl Cancer I* 1990; 82(13): 1107–1112.
66. Organisation for Economic Co-operation and Development (OECD). *Guidelines for testing of chemicals. No. 420: Acute oral toxicity—Fixed dose procedure*. Paris: Organisation for Economic Co-operation and Development, 2001.
67. Vietnam Ministry of Health. Guidelines for preclinical and clinical trials of traditional medicines, 2015 (in Vietnamese, issued with Decision No. 141/QD-K2DT dated October 27, 2015).
68. Lillo L, Pérez J, Muñoz I, et al. Production of exopolysaccharides by a submerged culture of an entomopathogenic fungus, *Metarhizium anisopliae*. *Rev Latinoam Quim* 2014; 42(1): 70–76.
69. Molnar K, Vas LM and Czigany T. Determination of tensile strength of electrospun single nanofibers through

- modeling tensile behavior of the nanofibrous mat. *Compos B Eng* 2012; 43(1): 15–21.
70. Jalalah M, Ahmad A, Saleem A, et al. Electrospun nanofiber/textile supported composite membranes with improved mechanical performance for biomedical applications. *Membranes* 2022; 12(11): 1158.
 71. Dubey P, Barker SA and Craig DQ. Design and characterization of cyclosporine A-loaded nanofibers for enhanced drug dissolution. *ACS Omega* 2020; 5(2): 1003–1013.
 72. Banik I. *Electrospinning nanofibers for controlled drug release*. Master's Thesis, University of Texas – Pan American, Edinburg, TX, 2013.
 73. Haroosh HJ, Dong Y, Jasim S, et al. Morphological structures and drug release effect of multiple electrospun nanofibre membrane systems based on PLA, PCL, and PCL/magnetic nanoparticle composites. *J Nanomater* 2022; 2022(1): 5190163.
 74. Hu J, Prabhakaran MP, Tian L, et al. Drug-loaded emulsion electrospun nanofibers: Characterization, drug release and in vitro biocompatibility. *RSC Adv* 2015; 5(121): 100256–100267.
 75. Laha A, Yadav S, Majumdar S, et al. In-vitro release study of hydrophobic drug using electrospun cross-linked gelatin nanofibers. *Biochem Eng J* 2016; 105: 481–488.
 76. AnjiReddy K and Karpagam S. Chitosan nanofilm and electrospun nanofiber for quick drug release in the treatment of Alzheimer's disease: In vitro and in vivo evaluation. *Int J Biol Macromol* 2017; 105: 131–142.
 77. Akrami HKM, Tayebi L and Ghorbani M. Curcumin-loaded naturally-based nanofibers as active wound dressing mats: Morphology, drug release, cell proliferation, and cell adhesion studies. *New J Chem* 2020; 44(25): 10343–10351.
 78. Sharma JN, Omran AA and Parvathy SS. Role of nitric oxide in inflammatory diseases. *Inflammopharmacology* 2007; 15: 252–259.
 79. Van VSF. Antimicrobial activity of South African medicinal plants. *J Ethnopharmacol* 2008; 119(3): 462–472.
 80. Liao TT, Shi YL, Jia JW, et al. Sensitivity of different cytotoxic responses of Vero cells exposed to organic chemical pollutants and their reliability in the bio-toxicity test of trace chemical pollutants. *Biomed Environ Sci* 2010; 23(3): 219–229.
 81. Mufidah M, Wahyudin E, Lawrence GS, et al. Cytotoxicity study of *Mezzetia parviflora* Becc. woodbark. *Trad Med J* 2013; 18(1): 35–37.